Coverage Analysis and Load Balancing in HetNets with mmWave Multi-RAT Small Cells

Gourab Ghatak[†] [‡], Antonio De Domenico[†], and Marceau Coupechoux[‡]

[†]CEA, LETI, MINATEC, F-38054 Grenoble, France; [‡]LTCI, Telecom ParisTech, Université Paris Saclay, France.
Email: gourab.ghatak@cea.fr; antonio.de-domenico@cea.fr, and marceau.coupechoux@telecom-paristech.fr

Abstract—We characterize a two tier heterogeneous network, consisting of classical sub-6GHz macro cells, and multi Radio Access Technology (RAT) small cells able to operate in sub-6GHz and millimeter-wave (mm-wave) bands. For optimizing coverage and to balance loads, we propose a two-step mechanism based on two biases for tuning the tier and RAT selection, where the sub-6GHz band is used to speed-up the initial access procedure in the mm-wave RAT. First, we investigate the effect of the biases in terms of signal to interference plus noise ratio (SINR) distribution, cell load, and user throughput. More specifically, we obtain the optimal biases that maximize either the SINR coverage or the user downlink throughput. Then, we characterize the cell load using the mean cell approach and derive upper bounds on the overloading probabilities. Finally, for a given traffic density, we provide the small cell density required to satisfy system constraints in terms of overloading and outage probabilities. Our analysis highlights the importance of deploying dual band small cells in particular when small cells are sparsely deployed or in case of heavy traffic.

I. INTRODUCTION

Future cellular networks will require a tremendous increase in data rates. This multi-fold enhancement cannot be achieved through incremental improvements on existing schemes [1]. For this, two techniques are particularly attractive: network densification using small cells [2] and mm-wave wave communications [3]. Densification of cellular networks consists of massive deployments of small cells, overlaying the existing macro cell architecture. Traditionally, small cells are deployed in sub-6GHz frequencies with the aim of offloading macro-cells. This calls for Inter-Cell Interference Coordination [4], [5] and load balancing [6]. To further increase the data rates, millimeter-wave (mm-wave) small cells, providing a very high bandwidth, are gaining popularity. Apart from the large bandwidths, mm-wave communication comes with highly directional antennas, which greatly reduces the co-channel interference [7]. Transmissions using higher frequencies suffer from larger attenuation and high sensitivity to blockages [8], [9]. The attenuation in mm-wave can be efficiently mitigated using beamforming techniques, with large number of antennas. As the wavelength is shorter, antennas are also smaller than in sub-6 GHz bands, so that deploying many more antennas becomes feasible. The highly directional antenna patterns pose in turn new issues in terms of coverage and user tracking. Moreover, providing initial access to standalone mm-wave base stations using beamtraining with thin beams presents a difficult challenge [10]. In this regard, the sub-6GHz band can be used to aid the initial access mechanism [11]. Specifically,

given suitable signal processing mechanisms, the position and orientation of the users relative to a sub-6GHz BS can be determined (see e.g., [12]). If sub-6GHz and mm-wave BS are co-located, or their position and orientation relative to one another are known, the coarse-grained angle information for beamtraining of the mm-wave RF front-end can be derived easily, which significantly speeds up the initial access procedure. As a result, it is unrealistic to assume ubiquitous coverage with only mm-wave small cells, and it is envisioned that multiple radio access techniques (RATs) will co-exist in future cellular networks [13] [14].

In this paper, we analyze the signal to interference plus noise ratio (SINR) distribution, the cell load and the downlink user throughput in a heterogeneous network with multi-RAT small cells using stochastic geometry. In order to optimize the user's SINR or to balance loads between tiers and RATs, we propose a cell association scheme based on two biases. In addition, we show the interest of deploying multi-RAT small cells to improve users' Quality of Service (QoS).

A. Related Work

Elsawy et al., have presented a comprehensive survey on stochastic geometry to model multi-tier cellular networks [15]. The SINR and physical data rate distributions have been derived in the literature by Bai et al. [16] for single-tier mm-wave networks, by Singh et al. [17] for multi-tier sub-6GHz and by Di Renzo for mm-wave networks [18]. In case of small cells operating in the same band of the macro cell, Singh et al. [17], have shown that, without advanced interference management techniques, the SINR decreases with increasing offloading bias. On the contrary, in this paper, we investigate how employing mm-wave in conjunction with sub-6GHz in small cells affects the system performance, and we show that optimizing the offloading biases can increase the user's SINR.

Omar et al. [19] have considered separate mm-wave and sub-6GHz BS. They characterized the blockage in a suburban context using real data from the Lancaster university, UK. The results provided by the authors are greatly limited since they use simulation studies in a specific scenario. These results may not be applicable in other network architectures. In the context of random networks, Yao et al. [20], similar to Di Renzo [18] have characterized the SINR coverage probability and the physical data rate in a multi-tier mm-wave network. However, the authors have not studied how traffic dynamics in a multi-user scenario impacts the network performance and

the average user throughput. On the other hand, Elshaer et al. [21] have analyzed a multi-tier network with sub-6GHz macro cells and mm-wave small cells. They have derived the SINR coverage probability as a function of the tier association bias, and they have shown only by simulations that a non-trivial optimal tier selection bias may exist. They have also investigated the relation between the association bias and throughput but without considering dynamic traffic. Moreover, they have characterized the load by using the average number of associated users in a cell; although, for a more realistic characterization, a dynamic traffic model should be considered. Furthermore, they have not optimized the user throughput while considering SINR outage constraints as well as overloading constraints.

In this perspective, Bonald and Proutière [22] have studied the relations between the traffic arrival rate and the cell load for a single cell scenario. In the case of single-tier cellular network, Blaszczyszyn and Karray [23] have approximated the cell load by a mean-cell approach to calculate the number of active users in a cell and the average user throughput. We leverage on these studies to design the optimal load balancing in multi-RAT heterogeneous networks and to derive bounds on overloading probabilities.

B. Contributions and Organization

The contributions of this paper can be summarized as follows:

1) SINR Coverage in a multi-RAT Heterogeneous Network: By using stochastic geometry, we derive the association probabilities and the SINR distribution of a typical user in a multi-RAT heterogeneous network with small cells operating in sub-6GHz and millimeter wave bands. In the literature, SINR coverage and throughput analyses have not been performed so far for such a system model.

2) Association Scheme for Tier and RAT Selection: We introduce a mechanism based on two biases, Q_T and Q_R, for tuning the tier and RAT selection, respectively. The principle of using biased received power for association has been used so far for tier offloading, whereas in this paper, we introduce a second bias to distribute the users between the available RATs in the small cells. Using these biases, we propose a two-step association scheme, in which initial access is performed in the sub-6GHz band. We compare our association mechanism with a more natural and exhaustive one-step association procedure in terms of sub-optimality of biased received power and downlink throughput. We show that this two-step association scheme fares better than cell association with beamtraining in mm-wave in terms of downlink throughput, specially in case of higher access delays.

3) Bias Optimization for SINR Coverage: Contrary to single-RAT heterogeneous networks, biasing the received power can lead to an improved SINR in a multi-RAT system. However, bias optimization is difficult in general. In the general case, Q_T and Q_R can be obtained by brute force if the range of possible values is small. To limit the complexity of this approach, we provide a strategy that sets Q_R based on the ratio of the approximated mean SINR in sub-6GHz band

and mm-wave. Thereafter, Q_T is obtained using a random-restart hill-climbing algorithm with adaptive step-size. We show that this strategy achieves near-optimal SINR coverage probability. We also highlight through simulations that sparse deployments require sub-6GHz band service for guaranteeing SINR requirements, whereas, in case of dense deployments, mm-wave may provide good SINR coverage, but with limited macrocell offloading. However, we show that, with large macrocell offloading, users at the edge of small cells, even in relatively dense deployments, need sub-6GHz band service to receive appreciable SINR coverage.

4) Cell Load Characterization and Load Balancing: Next, we analyze the effect of traffic density on the downlink user throughput by using a M/G/1/PS queue model. The existing literature in stochastic geometry defines the cell load as the average number of associated full buffer users, uniformly distributed over the cell area, see e.g., [15], [24]. This approach is static in nature and ignores the effect of dynamic traffic on the user distribution: users with low data rate tend indeed to stay longer in the system so that the user distribution becomes inhomogeneous in space. To account for this effect, we rely on results from queuing theory [22] and characterize the load of each cell by the mean cell approximation [23]. We solve a fixed point equation for the load to take the load of the interfering base stations into account. Accordingly, we derive upper bounds on the probability for a cell in each tier and RAT to become overloaded. Based on the derived bounds, we provide values of minimum necessary deployment densities required for a given traffic density so as to limit overloading and outage. We then derive and optimize the downlink user throughput with respect to tier and RAT biases under these constraints. We analyze the fundamental trade-off between user throughput, overloading and outage probabilities. We finally highlight that the capability of the small cells to operate also in the sub-6GHz band plays a key role to restrict outage, thereby justifying our system model.

The rest of the paper is organized as follows. In Section II, we introduce our two-tier heterogeneous network model. In Section III-B, we describe the proposed tier and RAT selection procedure and we derive the related association probabilities. Then, in Section IV, we compute and optimize the network downlink SINR distribution in terms of the tier and RAT selection biases. In Section V, we characterize the load of the network and the downlink user throughput under a dynamic traffic model, and, hence, we design the load balancing such that the user performance is maximized. Simulation results are provided in Section VI. Finally, the paper concludes in section VII. Main notations used in this paper are shown in Table I.

II. SYSTEM MODEL

A. Two-Tier Network Model

Consider a two-tier network consisting of macro BSs referred to as MBSs, and small cell BSs referred to as SBSs. MBSs are deployed to guarantee continuous coverage to the users. On the contrary, multi-RAT SBSs locally provide high data rate by jointly exploiting sub-6GHz and mm-wave bands. We also assume that the same sub-6GHz band is shared by

Table I: Notations and System Parameters

Notation	Parameter	Value
ϕ_M, λ_M	MBS process and density	λ_M = 5 per sq. km.
ϕ_S, λ_S	SBS process and density	λ_S = 5-200 per sq. km.
P_M, P_S	MBS/SBS power	46 dBm, 30 dBm
$\alpha_{tLr}, \alpha_{tNr}$	Approximated LOS/NLOS path-loss exponents	2, 4
G_0	Maximum directivity gain with mm-wave antenna	36 dB
N_0	Noise power density	-174 dBm/Hz
B_μ, B_{mm}	Sub-6GHz/mm-wave bandwidth	20 MHz, 1 GHz
$\sigma_{N,mm}^2, \sigma_{N,\mu}^2$	Noise power	$N_0 B_{mm}, N_0 B_\mu$
d_M, d_S	MBS/SBS LOS ball radius	200 m, 20 m
θ	Beamwidth	15 degrees

MBSs and SBSs. Therefore, users receiving services on this band experience both co-tier and cross-tier interference. MBS and SBS locations are modeled as independent Poisson point processes (PPP), ϕ_M and ϕ_S, with intensities λ_M and λ_S, respectively. Let the transmit power of MBS be given by P_M; the small cell transmit power, in both the bands, is assumed to be equal to P_S. End users are assumed to be distributed according to a PPP ϕ_U, independent of both ϕ_M and ϕ_S. Due to the independence of the PPPs and Slivnyak's theorem [15], without loss of generality, we carry out our downlink analysis considering a typical user located at the origin.

B. Blockage Processes

Cellular networks generally suffer from link blockages due to buildings, vehicles, etc. We assume a blockage process independent of the BS processes. Let the probability of a MBS and SBS to be in line of sight (LOS) with respect to the typical user at a distance r, be denoted by $p_M(r)$ and $p_S(r)$, respectively. For a given SBS, the LOS probability in sub-6GHz is assumed to be the same as that in mm-wave. This is because, the probability of a signal to be blocked mainly depends on the blockage process, which is independent of the carrier frequency [25]. Due to the blockages, MBSs and SBSs can be categorized into either LOS or NLOS (non line of sight) processes: $\phi_{ML}, \phi_{MN}, \phi_{SL}$, and ϕ_{SN}, respectively. The intensity of these modified processes are given by $p_M(r)\lambda_M$, $(1 - p_M(r))\lambda_M$, $p_S(r)\lambda_S$, and $(1 - p_S(r))\lambda_S$, respectively. In our work, we use the LOS ball approximation introduced in [16]. Accordingly, let d_M be the MBS LOS ball radius. The probability of the typical user to be in LOS from a MBS at a distance r is $p_M(r) = 1$, if $r < d_M$, and $p_M(r) = 0$, otherwise.[1] We assume a similar LOS ball for the SBS process with a different radius d_S.

C. Directional Beamforming in mm-wave

In case of mm-wave operations, the received powers take advantage of the directional antenna gain of the transmitter and the receiver. The user and the serving BS are assumed to

be aligned, whereas the interfering BSs are randomly oriented with respect to the typical user. Here, we assume a tractable model, where the product of the transmitter and receiver antenna gains, G, takes on the values a_k with probabilities b_k as given in Table 1 of [16]. Let the maximum value of G be G_0.

D. Path-loss Processes

We assume a distance based path-loss model where the path-loss at a distance d_{tvr} from a transmitter is given by: $l_{tvr}(d) = K_{tvr}d_{tvr}^{-\alpha_{tvr}}$ for a BS of type tvr, i.e., characterized by tier t (MBS or SBS), visibility state v (LOS or NLOS), and RAT r (sub-6GHz or mm-wave). Parameters K_{tvr} and α_{tvr} are derived from 3GPP UMa model for sub-6GHz MBSs, Umi model for sub-6GHz SBSs [27], and Umi model for mm-wave data transmission in SBSs [8]. By assuming a fast fading that is Rayleigh distributed with variance equal to one, the average received power is thus given by $P_{tvr} = P_t K_{tvr} d_{tvr}^{-\alpha_{tvr}}$, where P_t is the transmit power of a BS of tier t.

With our values (see Table I) of transmit powers, path-loss exponents, and LOS ball radii, we have $\frac{d_S^{\alpha_{SL\mu}}}{K_{SL\mu}P_S} \leq \frac{d_M^{\alpha_{ML\mu}}}{K_{ML\mu}P_M} \leq \frac{d_S^{\alpha_{SN\mu}}}{K_{SN\mu}P_S} \leq \frac{d_M^{\alpha_{MN\mu}}}{K_{MN\mu}P_M}$. The analysis in this paper is done considering that this ordering does not change even when powers are biased[2]. This assumption is reasonable considering that if a LOS BS exists and the tier bias is moderate, its biased received power is very likely to be greater than that of any NLOS BS. Accordingly, we analyze the performance of the network with tier-selection bias (Q_T) in the range: $1 \leq Q_T \leq \frac{d_S^{\alpha_{SN\mu}} K_{ML\mu} P_M}{d_M^{\alpha_{ML\mu}} K_{SN\mu} P_S} = Q_T^{max}$.

E. Dynamic Traffic Model

We consider a model in which users arrive in the system, download a file, and leave the system. Any new download by the same user is considered as a new user. The arrival process of the new users is Poisson distributed with an intensity λ [users $\cdot$s$^{-1}\cdot$m^{-2}] and these new users are uniformly distributed over the network area A. The average file size is σ [bits/user]. When there are n users simultaneously served by a base

---

[1]Note that the ball-based LOS probability model is not used in the literature for sub-6GHz frequencies. Instead, a model with LOS probability equal to 1 until a certain distance and then decreasing exponentially is preferred, see e.g., [26]. For simplicity and tractability reasons, we use here a step probability model following criterion 1 in [16] to make the connection between the two approaches.

[2]This assumption of ordering is considered only for the sake of simplicity and practicality. Considering higher bias values marginally alters the theoretical developments by modifying integral bounds in association probabilities. From an engineering point of view, very high bias values also lead to unacceptable outage probabilities and thus are of little interest.

station, the available resources are equally shared between them in a Round Robin fashion. Accordingly, we define the traffic density w in the network as $w = \lambda \cdot \sigma$ [bits·s^{-1}·m^{-2}]. Note that, while the user arrivals are uniform in space, as the space-time process evolves, users farther from the serving base stations which are characterized by lower data rates stay longer in the system, resulting in an inhomogeneous distribution of active users in the network.

III. CELL ASSOCIATION PROCEDURE

In this section, we propose a cell association scheme based on tier and RAT selection biases and we derive the corresponding association probabilities. We start below by a preliminary result.

A. Distribution of the Path-loss Process

To analyze the cell association, path-loss processes are reformulated as one dimensional processes, $\phi'_{tvr} = \{\xi_{tvr,i} : \xi_{tvr,i} = \frac{||x_i||^{\alpha_{tvr}}}{K_{tvr}P_t}, x_i \in \phi_{tv}\}$, $t \in \{M, S\}$, $v \in \{L, N\}$, $r \in \{\mu, m\}$. The processes ϕ'_{tvr} are non-homogeneous with intensities calculated as below.

Lemma 1. *The intensity measures of the LOS and NLOS path-loss processes, ϕ'_{tLr} and ϕ'_{tNr} are:*

$$\Lambda'_{tLr}(0, x) = \begin{cases} \pi\lambda_t(K_{tvr}P_t)^{\frac{2}{\alpha_{tLr}}} x^{\frac{2}{\alpha_{tLr}}}, & x < \frac{d_t^{\alpha_{tLr}}}{K_{tvr}P_t} \\ \pi\lambda_t d_t^2, & x > \frac{d_t^{\alpha_{tLr}}}{K_{tvr}P_t} \end{cases},$$

$$\Lambda'_{tNr}(0, x) = \begin{cases} 0, & x < \frac{d_t^{\alpha_{tNr}}}{K_{tvr}P_t} \\ \pi\lambda_t((K_{tvr}P_t x)^{\frac{2}{\alpha_{tNr}}} - d_t^2), & x > \frac{d_t^{\alpha_{tNr}}}{K_{tvr}P_t} \end{cases}. \quad (1)$$

Proof. The derivation of the intensity measure is similar to that in [28]. $\square$

The related intensities are obtained by differentiating the intensity measures, and are given by:

$$\lambda'_{tLr}(x) = \begin{cases} \frac{2\pi\lambda_t(K_{tvr}P_t)^{\frac{2}{\alpha_{tLr}}}}{\alpha_{tLr}} x^{\frac{2}{\alpha_{tLr}}-1}, & x < \frac{d_M^{\alpha_{tLr}}}{K_{tvr}P_t} \\ 0, & x > \frac{d_t^{\alpha_{tLr}}}{K_{tvr}P_t} \end{cases}$$

$$\lambda'_{tNr}(x) = \begin{cases} 0, & x < \frac{d_M^{\alpha_{tNr}}}{K_{tvr}P_t} \\ \frac{2\pi\lambda_t(K_{tvr}P_t)^{\frac{2}{\alpha_{tNr}}}}{\alpha_{tNr}} x^{\frac{2}{\alpha_{tNr}}-1}, & x > \frac{d_t^{\alpha_{tNr}}}{K_{tvr}P_t} \end{cases} \quad (2)$$

Lemma 2. *The probability density function (pdf) of the first point of $\phi'_{tv\mu}$, which corresponds to strongest sub-6GHz BS, is:*

$$f_{\xi_{tv\mu 1}}(r) = e^{-\Lambda'_{tv\mu}(0,r)} \lambda'_{tv\mu}(r).$$

Proof. The pdf of the first point in $\phi'_{tv\mu}$ is computed as

$$f_{\xi_{tv\mu 1}}(r) = \frac{d}{dr}\left[\mathbb{P}(\phi'_{tv\mu} \cap (0, r) = 0)\right] = \frac{d}{dr}\left[e^{-\Lambda'_{tv\mu}(0,r)}\right]$$
$$= e^{-\Lambda'_{tv\mu}(0,r)} \lambda'_{tv\mu}(r),$$

where $\Lambda'_{tv\mu}$ and $\lambda'_{tv\mu}$ are given by Eq. (1) and Eq. (2), respectively. $\square$

B. Tier and RAT Selection Scheme

For the cell association mechanism, we assume that BSs send their control signals in the sub-6GHz band. This is due to the fact that sub-6GHz communication benefits from a higher reliability and better coverage than mm-wave signals [29]. Our scheme is based on two biases Q_T and Q_R for selecting the tier and the RAT respectively, to which the user will be associated. Parameter Q_T is the classical cell range expansion parameter [17]: a user compares the strongest MBS signal with the strongest *biased* SBS signal. By varying Q_T, we are able to offload users from MBSs to SBSs. Once associated to a SBS, in our approach, a user compares the sub-6GHz received signal with the mm-wave signal strength *biased* with a second parameter Q_R. By varying Q_R, users can be distributed between RATs of the same SBS[3]. The association policy, summarized in Algorithm 1, consists of two steps: tier selection and RAT selection.

C. Tier Selection

The tier selection is based on the transmitted signal on the sub-6GHz band. As a result, a user can be served either by: 1. an MBS in LOS (ML), 2. an MBS in NLOS (MN), 3. an SBS in LOS (SL), or 4. an SBS in NLOS (SN). The biased received powers in sub-6GHz from the strongest LOS MBS, NLOS MBS, LOS SBS, and NLOS SBS are denoted as $P_{ML\mu 1}, P_{MN\mu 1}, Q_T P_{SL\mu 1}$, and $Q_T P_{SN\mu 1}$, respectively. User association is only based on measured biased received power. With the ordering assumption of Section II-D, however, a user associates with an NLOS BS only in absence of an LOS BS. It

---

Algorithm 1: Tier and RAT Selection

1: Measure downlink sub-6GHz received powers from all MBS, SBS.
2: Let $P_{Mv\mu 1}$ and $P_{Sv\mu 1}$ be the strongest powers received from an MBS and an SBS, resp.
3: **if** $P_{Mv\mu 1} \geq Q_T P_{Sv\mu 1}$ **then**
4:     Associate to the strongest MBS
5: **else**
6:     Associate to the strongest SBS
7:     Measure the mm-wave received power from the SBS (P_{Svm1}).
8:     **if** $P_{Sv\mu 1} \geq Q_R P_{Svm1}$ **then**
9:         Start service from SBS in sub-6GHz band.
10:     **else**
11:         Start service from SBS in mm-wave band.
12:     **end if**
13: **end if**

---

must be noted that the user does not know the visibility state of the base stations and associates only according to the biased received powers. The result that the user associates with an NLOS BS only in the absence of a LOS BS follows from the ordering described in Section II-D, which in turn, is a result of the values of the transmit powers and LOS ball radii. As a

---

[3]An alternative association scheme could be realized through the control of the SBS power in the different bands. However, as the transmit powers of SBSs are generally limited, we do not take this into consideration. Moreover, our approach can be easily adapted to study this alternative scheme.

consequence, for a LOS BS, the association probability of a typical user with tier t can be calculated as:

$$\mathbb{P}_{tL} = \mathbb{E}\left[\mathbb{1}(tL)\right] \cdot \mathbb{E}[\mathbb{1}(t'L)] \cdot \mathbb{P}(\tilde{Q}_T P_{tL\mu 1} > \tilde{Q}_{T'} P_{t'L\mu 1}) + \mathbb{E}\left[\mathbb{1}(tL)\right] \cdot (1 - \mathbb{E}[\mathbb{1}(t'L)]),$$
(3)

where $t, t' \in \{M, S\}$, $t \neq t'$, and $\mathbb{1}(.)$ is an indicator function: $\mathbb{1}(tL) = 1$ if and only if a point of tier t with visibility state L exists. The value of $\tilde{Q}_T$ is equal to 1 if $t = M$, else it is equal to Q_T. The first term of Eq. (3) is the product of the probabilities of 1) the existence of a LOS SBS and 2) the existence of a LOS MBS and 3) that the received power from the serving tier is greater than the one from the non-serving tier. The second term is the product of the probabilities of the existence of at least one LOS BS of the serving tier and the absence of a LOS BS of the non-serving tier. In the same way, for the NLOS BSs, we have:

$$\mathbb{P}_{tN} = (1 - \mathbb{E}[\mathbb{1}(t_M L)]) \cdot (1 - \mathbb{E}[\mathbb{1}(t_S L)]) \cdot \mathbb{P}(\tilde{Q}_T P_{tN\mu 1} > \tilde{Q}_T P_{t'N\mu 1}).$$
(4)

From these observations, we can deduce the tier selection probabilities as follows.

Lemma 3. *The tier selection probabilities are:*

$$\mathbb{P}_{ML} = \exp(-\pi\lambda_M d_M^2) \cdot \exp(-\pi\lambda_S d_S^2) \cdot W_1 + \exp(-\pi\lambda_M d_M^2) \cdot \left(1 - \exp(-\pi\lambda_S d_S^2)\right),$$

$$\mathbb{P}_{MN} = \left(1 - \exp(-\pi\lambda_M d_M^2)\right) \cdot \left(1 - \exp(-\pi\lambda_S d_S^2)\right) \cdot W_2,$$

$$\mathbb{P}_{SL} = \exp(-\pi\lambda_M d_M^2) \cdot \exp(-\pi\lambda_S d_S^2) \cdot (1 - W_1) + \exp(-\pi\lambda_S d_S^2) \cdot \left(1 - \exp(-\pi\lambda_M d_M^2)\right),$$

$$\mathbb{P}_{SN} = \left(1 - \exp(-\pi\lambda_M d_M^2)\right) \cdot \left(1 - \exp(-\pi\lambda_S d_S^2)\right) \cdot (1 - W_2),$$

where,

$$W_1 = \frac{(1 - e^{-(K_1+1)t_1})}{1 + K_1} + \exp(-\pi\lambda_S d_S^2) \cdot \left[\exp\left(-\Lambda'_{ML\mu}\left(0, \frac{d_S^{\alpha_{SL\mu}}}{Q_T K_{SL\mu} P_S}\right)\right) - \exp(-\pi\lambda_M d_M^2)\right],$$

$$W_2 = \exp(-\pi\lambda_S d_S^2)\frac{e^{-(K_2+1)t_2}}{1 + K_2},$$

$$K_1 = \pi\lambda_S\left(\frac{K_{SL\mu}P_S Q_T}{K_{ML\mu}P_M}\right)^{\frac{2}{\alpha_{SL\mu}}}(\pi\lambda_M)^{-\frac{\alpha_{ML\mu}}{\alpha_{SL\mu}}}, \quad t_1 = \pi\lambda_M(K_{ML\mu}P_M)^{\frac{2}{\alpha_{ML\mu}}}\left(\frac{d_S^{\alpha_{SL\mu}}}{Q_T K_{SL\mu} P_S}\right)^{\frac{2}{\alpha_{ML\mu}}},$$

$$K_2 = \pi\lambda_S\left(\frac{K_{SN\mu}P_S Q_T}{K_{MN\mu}P_M}\right)^{\frac{2}{\alpha_{SN\mu}}}(\pi\lambda_M)^{-\frac{\alpha_{MN\mu}}{\alpha_{SN\mu}}}, \quad and$$

$$t_2 = \pi\lambda_M d_M^2(K_{MN\mu}P_M)^{\frac{2}{\alpha_{MN\mu}}-1}.$$

Proof. See Appendix A. □

Lemma 4. *Given that a user is associated to a tier t of visibility state v, the pdf of the point in the 1D process of the serving BS is given by:*

$$\hat{f}_{\xi tv\mu 1}(x) = \frac{f_{\xi tv\mu 1}(x)}{\mathbb{P}_{tv}} \prod_{\forall(t'v' \neq tv)} \mathbb{P}(\phi'_{t'v'} \cap (0, x) = 0), \quad (5)$$

where $f_{\xi tv\mu 1}(x)$ is given by Lemma 2.

Proof. The proof follows from Lemma 3 above and Lemma 3 of [16]. □

D. RAT Selection in SBS

A dual-band user, associated with an SBS, is served using mm-wave if and only if the biased estimated power in the mm-wave band is larger than the power received in the sub-6GHz band.

Lemma 5. *Given that a user is associated with a SBS of visibility state v, the sub-6GHz and mm-wave RAT selection probabilities are respectively given by:*

$$\mathbb{P}_{v\mu} = \exp\left(-\pi\lambda_S\left(\frac{K_{Svm}G_0 Q_R}{K_{Sv\mu}}\right)^{\frac{2}{\alpha_{Svm}-\alpha_{Sv\mu}}}\right) \quad (6)$$

$$\mathbb{P}_{vm} = 1 - \mathbb{P}_{v\mu}. \quad (7)$$

Proof. See Appendix B. □

We denote $\mathbb{P}_{tvr} \triangleq \mathbb{P}_{tv}\mathbb{P}_{vr}$ as the association probability to a BS of type tvr with the convention that when $t = M$, $\mathbb{P}_{v\mu} = 1 - \mathbb{P}_{vm} = 1$.

E. Comparison to a One-Step Association Strategy

It must be noted that our proposed two-step association scheme is different from a more natural and exhaustive scheme (e.g., [21]), which directly compares the biased received powers from all the tiers and RATs (i.e., one-step procedure). In this regard, our two-step association procedure suffers from some sub-optimality with respect to the biased received power. However, access delay is lower with our strategy because the users position and orientation can be acquired in the sub-6GHz band before performing beamtraining.

First, we show that both the one-step strategy and our approach result in the same RAT selection, given that the user associates with the small cell tier. Then, our strategy differs from the one-step strategy when a user associates to an MBS while the biased power received from an SBS in mm-wave is higher than the biased power received from the MBS. We characterize hereafter the probability of this event.

Proposition 1. *If the typical user receives a higher sub-6GHz received power from an SBS S_1 as compared to an SBS S_2, then it also receives higher mm-wave power from S_1 than from S_2. Moreover, the tier selection and RAT selections biases Q_T and Q_R, do not impact this ordering of received powers.*

Proof. See Appendix D. □

From Proposition 1, we conclude that it is not possible for the typical user to have a higher received power in sub-6GHz band from SBS S_1 as compared to S_2 and lower mm-wave power from the same. Thus, the two schemes result in the same RAT selection, in case the user associates with the SBS tier. Therefore, the only difference in association arises when the biased received power from the strongest SBS (denoted S_1) in sub-6GHz band is less than that received from the strongest MBS (denoted by M_1), while simultaneously, the biased received power from S_1 in mm-wave is higher than the

biased received power from M_1. Let us call these events E_1 and E_2, respectively. This results in sub-optimal association of some users in the sense that these users are not associated to the tier-RAT pair providing the highest biased power. We have the following result to model this sub-optimal association.

Lemma 6. *The probability of suboptimal association in case of an association with LOS MBS instead of mm-wave LOS SBS is given as:*

$$\mathbb{P}_{SO} = 2\pi\lambda_M \frac{1 - \exp\left(-\pi\left(\lambda_S\zeta_2 - 2\lambda_S\zeta_1 + \lambda_M\right)d_M^2\right)}{2\zeta_2}, \quad (8)$$

where $\zeta_1 = \frac{P_S Q_T}{P_M}$ *and* $\zeta_2 = \frac{K_m P_S Q_R Q_T}{K_\mu P_M}$

Proof. See Appendix E. $\qquad\square$

In Section VI, we provide numerical results to show that the sub-optimality is limited, and this loss can be compensated by a faster access procedure, which may increase the network throughput.

F. A Simple Strategy to Prioritize mm-Wave RAT

Depending on the network load and the active services, the mobile operator may want to prioritize one RAT over the other. For instance, the utilization of mm-wave frequencies for latency sensitive applications, can be an attractive strategy to offload the sub-6GHz band, which can mainly be dedicated to communications requiring reliability and continuous service. In the following, we propose a strategy to achieve this goal. For that, we introduce the following definition:

Definition 1. *The critical distance with respect to the typical user is the distance of the SBS from which the typical user receives equal mm-wave and sub-6GHz power.*

For our system model, the critical distance for the LOS SBS tier can be expressed as:

$$d_{CL} = \left(\frac{K_{SLm}}{K_{SL\mu}}G_0\right)^{\frac{1}{\alpha_{SLm} - \alpha_{SL\mu}}} \quad (9)$$

Proposition 2. *If there exists exactly one point of the LOS SBS process within the critical distance, the typical user always selects mm-wave as serving RAT. Moreover, in this scenario, this is the optimal strategy in terms of SINR for the typical user.*

Proof. In the case where this condition holds, the useful signal received in mm-wave is greater than that received in sub-6GHz (as per definition of d_{CL}). Thus, the typical user always selects the mm-wave RAT from the serving SBS. Moreover, as all interfering LOS SBS are outside d_{CL}, the sub-6GHz interference has state-wise dominance with respect to the mm-wave interference. Hence, the mm-wave SINR is always larger than the sub-6GHz SINR. $\qquad\square$

From Eq. (9), we see that, for given path-loss exponent values of each user, the critical distance can be controlled by varying the product of the transmitter and receiver antenna gain G_0. This enables the users served by LOS SBSs to adjust their antenna gain in order to select mm-wave communications, and ensure that this choice is optimal from the SINR

perspective. In addition, given a fixed antenna gain G_0, we have the following corollary, which provides the deployment density of SBSs that maximizes the probability of occurrence of a single LOS SBS within the critical distance.

Corollary 1. *The maximum probability of occurrence of exactly one point of LOS SBS within the critical distance is $1/e$, and this occurs at:*

$$\lambda_S = \frac{1}{\pi}\left(\frac{K_{Svm}}{K_{Sv\mu}}G_0\right)^{\frac{2}{\alpha_{SL\mu} - \alpha_{SLm}}}.$$

Proof. The probability of existence of only one point within the critical distance is calculated as:

$\mathbb{P}\left(\phi'_{SL} \cap b(0, d_{CL}) = 1\right) = \pi\lambda_S d_{CL}^2 \exp(-\pi\lambda_S d_{CL}^2)$,

where $b(0, d_{CL})$ is the ball of radius d_{CL} centered at the origin. The maximum value of this probability occurs at $\pi\lambda_S d_{CL}^2 = 1$, then substituting the value of d_{CL} from Eq. (9) completes the proof. $\qquad\square$

IV. DOWNLINK SINR DISTRIBUTION

In this section, we first derive the downlink SINR coverage probability for the maximum biased received power association policy and then optimize the biases with respect to the cell coverage.

A. SINR Coverage Probability

The SINR coverage probability at a threshold γ, can be expressed as $\mathbb{P}_C(\gamma) = \mathbb{P}(SINR > \gamma)$. Following the theorem of total probabilities, we have:

$$\mathbb{P}_C(\gamma) = \sum_{t \in \{M,S\}, \, v \in \{L,N\}, \, r \in \{\mu,m\}} \mathbb{P}(SINR_{t,v,r} > \gamma | t, v, r)\mathbb{P}_{tvr}, \quad (10)$$

We divide the problem of finding the overall coverage probability into two parts: the one related to the sub-6GHz service and the one associated with the mm-wave service, and we compute the coverage probability by relying on 1D processes ϕ'_{tvr}.

Lemma 7. *The conditional SINR coverage probability, given that the user is associated with a sub-6GHz BS of tier t and visibility state v, is given by:*

$$\mathbb{P}_{Ctv\mu}(\gamma) = \int_0^\infty \exp\left(-\gamma \cdot \sigma_{N,\mu}^2 \cdot x - \sum_{t',v'} A_{t'v'}(\gamma, x)\right) \hat{f}_{\xi tv\mu 1}(x)dx, \quad (11)$$

where,

$$A_{t'v'} = \int_{l_{t'}}^\infty \frac{\gamma x}{y + \gamma x}\Lambda'_{t'v'\mu}(dy), \quad \forall \, t' \in \{M,S\}, v' \in \{L,N\}.$$

Additionally, $l_{t'} = x$ *if* $t' = t$, $l_{t'} = Q_T \cdot x$, *when* $t = M$ *and* $t' = S$, *and* $l_{t'} = x/Q_T$, *when* $t = S$ *and* $t' = M$.

Proof. See Appendix C. $\qquad\square$

Lemma 8. *The conditional SINR coverage probability, given that the user is associated with a SBS in mm-wave of visibility state v, is given by:*

$$\mathbb{P}_{CSvm}(\gamma) = \int_0^\infty \exp\left(-\frac{\gamma \cdot x \cdot \sigma_{N,mm}^2}{G_0} - B_1(\gamma, x)\right.$$
$$\left. - B_2(\gamma, x)\right) \hat{f}_{\xi Svm1}(x)dx, \qquad (12)$$

$$\text{with} \quad B_1(\gamma, x) = \sum_{k=1}^4 \left(-b_k \int_x^\infty \left(\frac{a_k \gamma x}{y + a_k \gamma x} \Lambda'_{Svm}(dy)\right)\right),$$

$$\text{and,} \quad B_2(\gamma, x) = \sum_{k=1}^4 \left(-b_k \int_x^\infty \left(\frac{a_k \gamma x}{y + a_k \gamma x} \Lambda'_{Sv'm}(dy)\right)\right).$$

Proof. The proof follows in a similar way to that of Lemma 7. □

B. A Near-Optimal Strategy for Bias Selection

On the one hand, obtaining optimal biases with respect to the SINR coverage probability is difficult because of the complex expressions. On the other hand, using brute force to search through all the possible pairs of tier and RAT selection biases can have a very high time-complexity which limits practical implementation. Accordingly, in this section, we propose a strategy to select the tier and RAT selection biases with the aim of maximizing the SINR coverage.

Specifically, the proposed strategy is based in two parts: 1) computing the RAT selection bias, Q_R and 2) obtaining the tier selection bias Q_T based on a random-restart hill-climbing algorithm.

1) Heuristic for Selection of Q_R: The heuristic to set the RAT selection bias Q_R consists of computing the ratio of the mean signal to interference and noise perceived by the typical user on the sub-6GHz and mm-wave bands. That is:

$$Q_R = \frac{\mathbb{E}\left[\frac{S_{mm}}{I_{mm} + \sigma_{N,mm}^2}\right]}{\mathbb{E}\left[\frac{S_\mu}{I_\mu + \sigma_{N,\mu}^2}\right]}, \qquad (13)$$

where I_μ and I_{mm}, respectively, are the sum of the interference from all the (LOS and NLOS) BSs in sub-6GHz and mm-wave, respectively. It must be noted that evaluating the above expression without the knowledge of the coverage probability is not possible. However, with a relaxation of independence of the useful signal and the interference for each of the RATs, the expected values can be approximated using the results of [30]. Once Q_R is computed, Q_T can be obtained by the following step

2) Random-Restart Hill-Climbing Algorithm for Selection of Q_T: We start with a random value of Q_T, i.e., Q_T^0 and calculate the gradient of $\mathbb{P}_C$ at Q_T^0. In case the gradient is non-negative, we increase the value of Q_T by a step size of k. If the gradient is negative, we decrease the value of Q_T by the same step size k. We continue this procedure with the updated value of Q_T until the variation in Q_T is sufficiently small. In the case where the product of two consecutive values of the gradient is non-positive, and as a result we cross a stationary

point, we reduce the step size by a factor β and continue the algorithm.

In our algorithm, Q_T^{max} is the maximum value of the bias in the moderate range. If the coverage probability is monotonic, quasi-convex or quasi-concave, this procedure provides the optimal value of Q_T. In the general case, the procedure stops at a local maximum in the range $1 \leq Q_T \leq Q_T^{max}$. This local maximum can be improved by repeatedly starting the same algorithm with random starting points. This procedure to obtain Q_T is summarized in Algorithm 2. In Section VI, we compare the performance of this proposed scheme with the optimal case.

Algorithm 2: Random-restart hill-climbing algorithm with Adaptive Step-Size

---

1: Set $t = 1$, $k > 0$, $\epsilon > 0$ and $\beta > 1$.
2: Set $Q_T(0) = Q_T^0$.
3: **while** $|Q_T(t) - Q_T(t-1)| > \epsilon$ **do**
4:     **if** $\frac{d\mathbb{P}_C}{dQ_T}(Q_T(t)) > 0$ **then**
5:         $Q_T(t) = \min\{Q_T(t-1) + k, Q_T^{max}\}$.
6:     **else**
7:         $Q_T(t) = \max\{Q_T(t-1) - k, 1\}$.
8:     **end if**
9:     **if** $\frac{d\mathbb{P}_C}{Q_T}(Q_T(t)) \cdot \frac{d\mathbb{P}_C}{Q_T}(Q_T(t-1)) < 0$ **then**
10:         $k \leftarrow \frac{k}{\beta}$.
11:     **end if**
12:     $t \leftarrow t + 1$
13: **end while**

V. CELL LOAD, USER THROUGHPUT, AND LOAD BALANCING

In the previous section we have focused only on coverage aspects, we now take into account cell loads to show how tier and RAT selection biases can improve the user average throughput. For this, we consider a multi-user system where the users share the available radio resources according to a round robin policy.

A. Cell Load Characterization

According to our model of the traffic arrival process, the traffic density is given as $w = \lambda \cdot \sigma$ [bits/s/m²]. For a single cell scenario, Bonald et al. [22] have modeled the load of the cell of area A as $\rho = \int_A \frac{w}{R(s)}ds$ [22], where $R(s)$ is the physical data rate of a user located at s. In case of Poisson-Voronoi cells, the average load is generally difficult to evaluate because of the randomness in the shape and sizes of the cells. Furthermore, in a multi-cell scenario, the load of a cell depends on the SINR characteristics of the cell, which in turn, depends on the load of the other cells in the network.

We know from the ergodicity of the PPP, that the fraction of the BS of type tvr that are idle is equal to the fractional idle time of the typical BS of same type. Accordingly, assuming that the load of the typical BS of type tvr is given by $\bar{\rho}_{tvr}$, then, the fraction of idle BS of type tvr is given by $1 - \bar{\rho}_{tvr}$. We substitute this value $\forall\, t, v, r$ in the calculation of the load as:

$$\bar{\rho}_{tvr} = \int_\gamma \frac{wA_{tvr}}{B_r \log_2(1 + \gamma)} p_{tvr}(\bar{\rho}, \gamma)d\gamma, \qquad (14)$$

where the pdf of the SINR $p_{tvr}(\bar{\rho}_{tvr}, \gamma)$ is a function of the average idle fraction of the BS and $\bar{\rho}$ is a vector of the fraction of idle BSs of all BS types, i.e., $\bar{\rho} = [\rho_{tvr}] \, \forall \, t, v, r$. This fixed point equation is then solved in an iterative manner to obtain the actual load of the BS of all the tiers (starting from zero load). Then, the SINR coverage probability with $1 - \bar{\rho}$ fraction of BSs idle, given that the user is associated with a sub-6GHz BS of tier t and visibility state v, is given by:

$$\mathbb{P}_{Ctv\mu}(\bar{\rho}, \gamma) = \int_0^\infty \exp\left(-\gamma \cdot \sigma_{N,\mu}^2 \cdot x - \right.$$
$$\left. \sum_{t',v'} A_{t'v'}(\gamma, x, \rho_{t'v'\mu})\right) \hat{f}_{\xi tv\mu 1}(x) dx, \quad (15)$$

where,

$$A_{t'v'}(\gamma, x, \rho_{t'v'\mu}) = \int_{l_{t'}}^\infty \frac{\gamma x}{y + \gamma x} \Lambda'_{t'v'\mu}(dy, \rho_{t'v'\mu}),$$
$$\forall \, t' \in \{M, S\}, v' \in \{L, N\}.$$

Additionally, $l_{t'} = x$ if $t' = t$, $l_{t'} = Q_T \cdot x$, when $t = M$ and $t' = S$, and $l_{t'} = x/Q_T$, when $t = S$ and $t' = M$. The intensity measures Λ_{tvr} are obtained by modifying λ_t to $\lambda_t \rho_{tvr}$ for each BS type. The calculation for the mm-wave BS follows in the same way.

It should be noted that in case of a Poisson distributed network, there exists a non-zero fraction of unstable cells ($\rho \geq 1$), which cannot handle their load.

Lemma 9. *The probability of a typical cell of type tvr to be unstable is bounded as:*

$$\mathbb{P}\left(\rho_{tvr} \geq 1\right) \leq \min\left\{\frac{\sigma_{tvr}^2}{(1 - \bar{\rho}_{tvr})^2}, \bar{\rho}_{tvr}\right\}, \quad (16)$$

where $\sigma_{tvr}^2 = \mathbb{E}[\rho_{tvr}^2] - \bar{\rho}_{tvr}^2$, is the variance of the load, which can also be calculated, similar to $\bar{\rho}_{tvr}$ by using the SINR coverage probability of the typical user.

Proof. We have for every $k > 0$,

$$\mathbb{P}\left[(\rho_{tvr} - \bar{\rho}_{tvr} \geq k\sigma_{tvr})\right] \leq \mathbb{P}\left[|\rho_{tvr} - \bar{\rho}_{tvr}| \geq k\sigma_{tvr}\right] \overset{(a)}{\leq} \frac{1}{k^2},$$

where, (a) is from Chebyshev inequality. Substituting $k \cdot \sigma_{tvr} = 1 - \bar{\rho}_{tvr}$, we obtain the first term of the right hand side in (16). The second term is a direct result of Markov inequality. □

B. Average User Throughput

The average downlink throughput that a user receives from a BS of type tvr is $T_{tvr} \overset{\Delta}{=} \frac{wA_{tvr}}{N_{tvr}}$, where N_{tvr} is the average number of active users in a cell, which can be approximated by using the mean cell approach [23]. The mean cell is defined as a hypothetical cell that has the same average load as that of a typical cell.

Lemma 10. *The downlink average user's throughput in a non-overloaded mean cell of type tvr is:*

$$T_{tvr} = \lambda \cdot \sigma \frac{1 - \bar{\rho}_{tvr}}{\bar{\rho}_{tvr}} A_{tvr}.$$

Proof. The proof is similar to that presented in [22]. □

The average user throughput is then given by theorem of total probability as: $T = \sum_{tvr} \mathbb{P}_{tvr} T_{tvr}$. Due to the different operating bandwidths, the bias values which provide the optimal user throughput may lead to weak SINR, which in turn increases the outage. Thus, to guarantee the communication reliability, it is necessary to consider an SINR constraint on the selection of the optimal biases. We define the outage probability with respect to a SINR threshold $\gamma_{\min}$ as:

$$\mathbb{P}_{o,tvr}(\gamma_{\min}) = 1 - \mathbb{P}_{Ctvr}(\gamma_{\min}). \quad (17)$$

Therefore, we introduce the notion of effective throughput, which measures the throughput of the users, which are not in outage, as: $T_{eff}(\gamma_{\min}) = \sum_{tvr} \mathbb{P}_{tvr} \cdot T_{tvr} \cdot \mathbb{P}_{Ctvr}(\gamma_{\min})$. In Section VI, we optimize Q_T and Q_R so as to maximize the average effective user throughput $T_{eff}(\gamma_{\min})$ under the constraint of a maximum outage probability $\mathbb{P}_{o,tvr}(\gamma_{\min}) \leq \bar{\mathbb{P}}_o$ for every BS type tvr.

C. Delay-Throughput Trade-off of the One-Step Association Scheme.

It must be noted that the sub-optimality in biased received power does not always deteriorate the downlink user throughput, specially for larger access delays. To illustrate this, let us assume that the initial access using mm-wave suffers from a delay given by Δ. In this regard, the throughput for the users associated to the SBSs in mm-wave RAT is given by:

$$T_{Svm} = \frac{\sigma}{\frac{N_{Svm}}{\Lambda} + \Delta}, \quad (18)$$

where $\Lambda = \lambda \cdot A_{Svm}$ is the traffic arrival rate in terms of users per second in the mm-wave cell of visibility state v of coverage area $A_{Svm} = \frac{\mathbb{P}_{Svm}}{\lambda_S}$, $N_{Svm} = \frac{\bar{\rho}_{Svm}}{1 - \bar{\rho}_{Svm}}$ is the number of active users in the cell, and $\frac{N_{Svm}}{\Lambda}$ is the transmission time according to Little's theorem [31]. In Section VI, we provide some numerical results to show that in case of realistic access delay with the mm-wave RAT, our scheme performs better in terms of the downlink throughput.

VI. SIMULATION RESULTS

In this section, we first validate our path-loss exponent approximation with respect to 3GPP values. Then, we study the effects of biases on SINR and user throughput. Finally, we discuss the selection of optimal biases.

A. Validation of the Path-loss Exponent Approximation

Fig. 1 shows the comparison of our analytical results using the approximated path-loss exponents from Table I (see Eq. 9) with Monte-Carlo simulations with actual path-loss exponents from the 3GPP recommendations [8], [27] in terms of SINR coverage probability for various tier, RAT selection biases, and density values. Our results indicate that the analytical expressions based on approximated path-loss exponents provide good approximations to the simulated results with 3GPP values of exponents. Hence, this approximation can be used for analyzing the system performance.
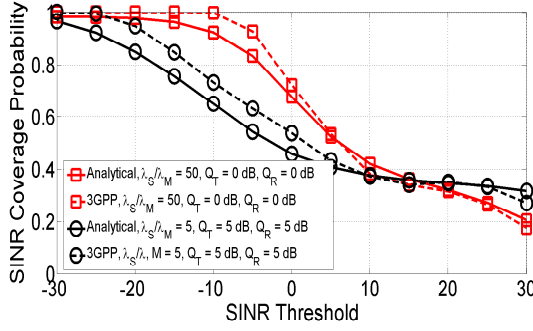
Figure 1: Validation of the approximated path-loss exponents with 3GPP parameters.

B. Trends in Cell Association Probabilities

Fig. 2 (left) shows the tier selection probabilities with respect to the ratio of the MBS and SBS densities λ_S/λ_M with $Q_T = 10$ dB and with $Q_T = 0$ dB. As expected, the association to MBSs decreases as λ_S/λ_M increases or when Q_T increases. However, the association to LOS BSs does not change appreciably when increasing Q_T from 0 to 10 dB. Only cell edge users, which are more likely to be in NLOS visibility, are indeed affected by moderate values of Q_T.

The conditional probability of mm-wave service, given that the user has associated with a SBS, is plotted in Fig. 2 (right), by varying Q_R for two different antenna gains and deployment density ratios. As expected, this probability increases with Q_R. However, it is interesting to note that the maximum directional antenna gain has a large effect on the RAT selection regardless of the SBS density. For example, increasing by only 3 dB the antenna gains of transmitter and receiver each has much more impact on the mm-wave association than deploying four times more SBSs.

C. Comparison with the One-Step Association Strategy:

We plot the probability of sub-optimal association (8) in the left side of Figure 3, for various tier and RAT selection biases and two antenna gains. We note that the probability of sub-optimal association is low ($\leq 12\%$). Moreover, the probability becomes negligible with low tier selection bias ($\leq 1\%$). This is because with lower Q_T, the biased received power of the mm-wave transmission in SBS are lower, thereby reducing the probability of sub-optimality. Similarly, with lower antenna gain (G_0), the biased mm-wave power is lower, resulting in low sub-optimality. Furthermore, we observe that the probability of sub-optimal association increases with increasing network densification, since denser networks correspond to higher mm-wave powers. However, for $G_0 = 30$ dB, the probability of sub-optimal association does not exceed 8% even for very dense deployments.

In the right side of Figure 3, we compare the throughput perceived by the typical user with the two approaches (18). We plot the downlink user throughput vs the initial access delay Δ, for two different file sizes (σ). We see that with increasing Δ, the throughput with the one-step association scheme decreases, and goes below the throughput achieved by using our two-step

solution. In practical systems, the initial access delay in mm-wave can be of the order of several milliseconds [10]. As a result, our two step association is more efficient in terms of the user throughput as compared to the case where association is performed in one-step.

D. Trends in SINR Coverage Probabilities

In Fig. 4, we plot the SINR coverage probability of the typical user, with respect to Q_T and various ratios of SBS to MBS densities. In the case where the SBSs operate only in sub-6GHz band, i.e., $Q_R = -\infty$ dB (Fig. 4 left), increasing the tier selection bias decreases the SINR coverage probability because some users are forced to associate with BSs providing less signal power. For $d_M = 200$ m and $d_S = 20$ m, Fig. 4 (right) shows that the same effect can be observed when SBSs transmit data only in mm-wave, i.e., $Q_R = \infty$, regardless of the deployment densities.

However, in the latter case, when varying the blockage characteristics, we observe two different behaviors for the SINR coverage probability. In Fig. 5, we see that depending on the LOS ball radii, the SINR may increase with the tier selection bias. Indeed, the SINR may improve by associating macro cell users to SBSs transmitting data only in mm-wave, even though this SBS offers less power in sub-6GHz band, because the received power in mm-wave may be higher due to antenna gain. Additionally, the interference in mm-wave is generally lower than the one in the sub-6GHz band. However, increasing the bias further forces the users closer to the MBS to associate with a SBS that provide very limited received power, which leads to lower SINR.

Assuming maximum power tier selection ($Q_T = 0$ dB), Fig. 5 (right) shows that increasing Q_R has contrasting effects on the SINR depending on the ratio of SBS to MBS densities. Increasing the SBS density increases co-channel interference more in sub-6GHz than in mm-wave. Moreover, as the user-SBS distance decreases, the useful signal power increases more in mm-wave than in sub-6GHz. Both effects are due to the difference in the path-loss models. As a consequence, as the SBS density increases ($\lambda_S/\lambda_M = 200$), it is more and more attractive for a user to be served by mm-wave band, which is realized by higher values of Q_R. On the contrary, in case of sparser SBS deployments ($\lambda_S/\lambda_M = 15, 50, 100$), increasing Q_R forces users to be served from distant SBSs in mm-wave, and the gain due to the reduced interference cannot compensate the signal strength loss. Note that this contrasting effect cannot be observed with single RAT networks.

We now study the joint effect of Q_T and Q_R for dense ($\lambda_S/\lambda_M = 200$) and sparse ($\lambda_S/\lambda_M = 50$) deployments in Fig. 6 left and right, respectively. For sparse SBS deployments, the conclusions drawn so far hold: high SINR regions occur at low Q_T and Q_R. The optimum biases as marked in the figure are $Q_T = 0$ dB and $Q_R = 0$ dB. For dense deployments, however, we can observe that, for a high Q_T (here for $Q_T > 8$ dB), SINR coverage probability generally decreases with increasing Q_R, which is in contrast to the case when Q_T is small. This is because, for users far away from their serving SBS, it is now preferable to get associated with sub-6GHz than
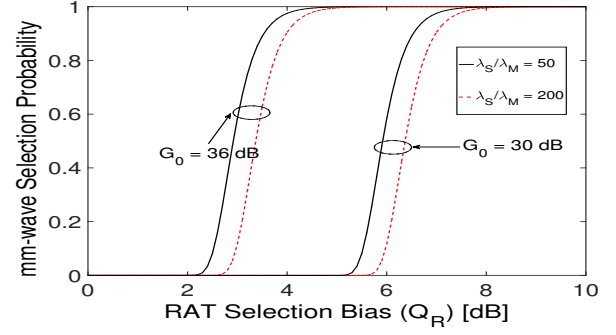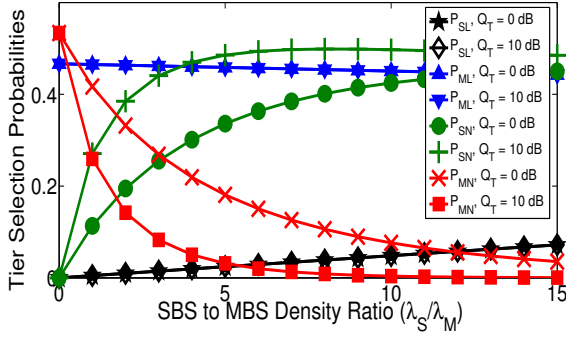
Figure 2: left) Tier selection probability; right) Conditional mm-wave RAT selection probability with 3GPP parameters.
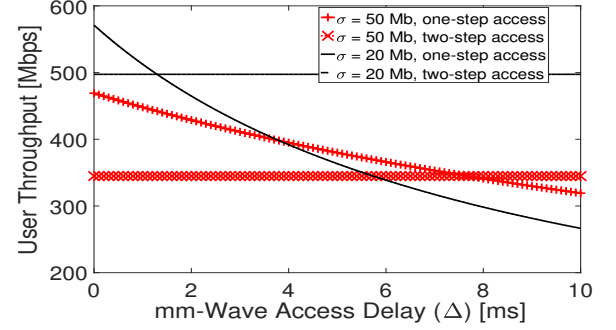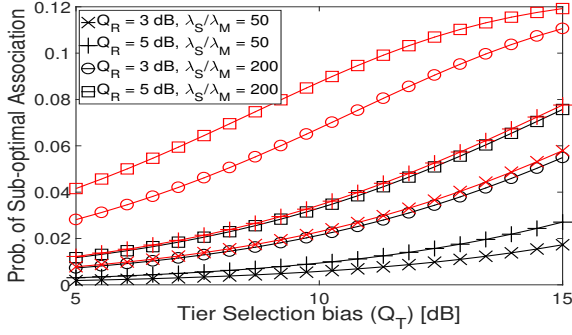

Figure 3: left) Probability of sub-optimal association for different Q_R and for different $\frac{\lambda_S}{\lambda_M}$. The black curves correspond to $G_0 = 30$ dB and the red curves correspond to $G_0 = 36$ dB; right) Delay-throughput trade-off with mm-wave initial access; $G_0 = 36$ dB, $Q_T = 10$ dB, $Q_R = 5$ dB, $\lambda = 100$ [user $\cdot$ km^{-2} s^{-1}].
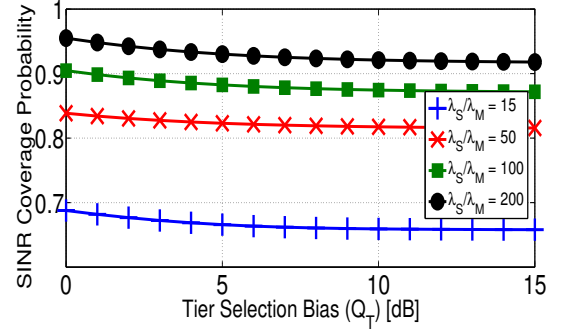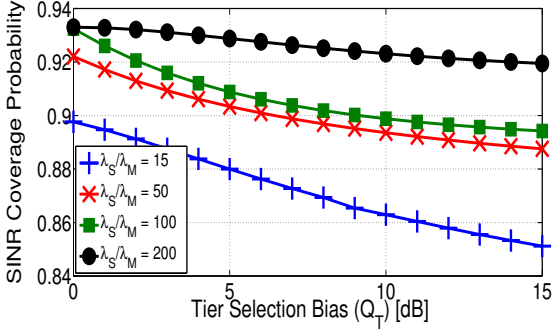

Figure 4: SINR coverage probability vs tier selection bias at a threshold of $\gamma = -10$ dB for left) $Q_R = -\infty$ dB; right) $Q_R = \infty$, $d_M = 200$ m, $d_S = 20$ m.
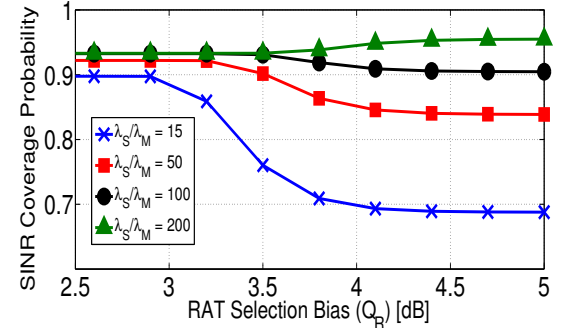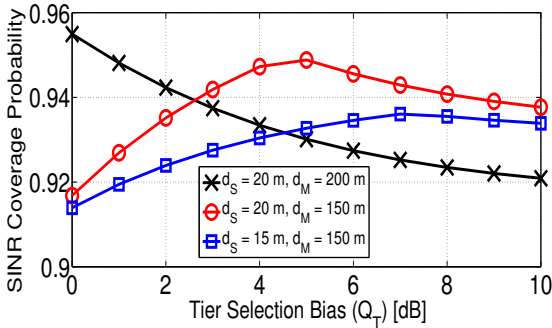
Figure 5: left) SINR coverage probability with different LOS radii for $Q_R = \infty$, $\lambda_S/\lambda_M = 200$; right) SINR coverage probability vs RAT selection bias with $Q_T = 0$ dB.

with mm-wave. The optimal biases in this case are $Q_T = 0$ dB and $Q_R = 5$ dB.

E. Performance of the Near-Optimal Strategy to Select Tier and RAT Biases

In Section IV-B, we have proposed a near-optimal strategy to fix the RAT and tier-selection bias, to reduce the complexity of the brute force search. In this strategy, first Q_R is selected according to (13). Then, for the fixed Q_R, a Q_T is selected according a random-restart hill-climbing algorithm as described in Algorithm 2. We show the convergence of the algorithm in the left side of Fig. 7 for $\lambda_S/\lambda_M = 200$ and for two pairs of LOS radii. With $k = 0.5$ and $\beta = 2$, the proposed algorithm converges at $Q_T = 3.19$ dB for $d_S = 20$ m and $d_M = 150$ m, and at $Q_T = 7.16$ dB for $d_S = 15$ m and $d_M = 100$ m. Fig. 7 (center) compares various bias selection strategies. We observe that our proposed strategy performs at least as good as the classical strategy based on the maximum received power. In particular, for sparse deployment of SBSs, the proposed strategy and the maximum power association perform equal to the optimal association. However, with increasing SBS density, the performance of the maximum power association decreases due to the increasing interference in the sub-6GHz RAT. On the contrary, since our strategy takes interference into account, it achieves near optimal SINR.

F. Analysis of the Bound on Overloading Probabilities

In this section, we investigate the relation between the cell overloading probabilities and the traffic density, based on the analytical bound derived in Lemma 9. We see in Fig. 7 (right) for $\lambda_S/\lambda_M = 5$ that the proposed bound is relatively loose but it provides the operator the guarantee that the overload probability will not exceed this value. Based on this bound and a constraint on the overall outage probability, a conservative network sizing can be derived. In Fig. 8 (left), we show the minimum deployment density required such that feasible biases exist to meet both theses constraints. The more stringent the constraints are, the more SBSs the operator should deploy. When the traffic density is low, the outage probability is the limiting constraint and accordingly, the minimum deployment density is the one required to maintain coverage. However, as traffic density increases, overloading probability is determining.

G. Rate Optimal Choice of Tier and RAT Selection Biases

In this section, we optimize tier and RAT selection biases with respect to the average effective throughput. To guarantee a good coverage, we impose a constraint on the outage probability (from 7.5 to 12.5%[4]). The MBS association probability corresponding to the optimal Q_T as a function of the traffic density is shown in Fig. 8 (right). Depending on the ratio of densities λ_S/λ_M, users are offloaded from MBS to SBS (for low SBS densities) or vice-versa (for high SBS densities).

[4]Note that generally, PPP based modeling of cellular networks provide a pessimistic view of the network. Previous studies showed that an outage of 1% in hexagonal model corresponds to 10% outage in a PPP based modeling for the same network parameters [32].

In Fig. 9 (left), we show the optimal effective downlink throughput as a function of the traffic density for various deployment densities and outage constraints. We observe that more stringent outage constraints result in lower downlink throughput in the network. This is because biases are mainly optimized to guarantee coverage also for cell edge users. We also observe that increasing the SBS density not only results in higher throughput, but also increases the range of traffic densities that the network can serve, i.e., the network capacity. In this evaluation, we have obtained the downlink throughput by considering that the users in overloaded base stations receive zero throughput. Therefore, even though the network as a whole can serve traffic densities up to 1 Gbps/m^2, the MBS tier gets overloaded for much lower traffic densities. Accordingly, the network is no longer well-dimensioned for the region of traffic densities beyond the MBS overloading points. Furthermore, in Fig. 9 (right), we plot the optimum association probabilities as a function of outage probability with $\lambda_S/\lambda_M = 50$ and traffic density of 200 bits·s^{-1}m^{-2}. We see that for more stringent outage constraints, sub-6GHz service in SBSs becomes necessary, in addition to mm-wave service, to satisfy the QoS constraints of outage and overloading simultaneously, thus justifying the interest of deploying dual band SBSs.

As a conclusion, in dense SBS deployments (see Fig. 10, right), the users do not suffer from outage even in the case of high tier biases. In this case, Q_R should be high enough to maximize the mm-wave association probability. In case of $\lambda_S/\lambda_M = 200$, this results in a maximum throughput of around 30 Gbps at $Q_T = 10$ dB and $Q_R = 6$ dB. In sparse SBS deployments (Fig. 10 (left)), high values of Q_T are desirable to offload traffic from overloaded MBSs. However, as the SBS ranges increase, mm-wave becomes unattractive for users at the SBS cell edges. We can observe that increasing Q_R beyond a certain limit pushes the SBS users in outage thereby decreasing the effective throughput. The maximum average throughput in this scenario, considering the regime of biases where the MBS tier is not overloaded, is 10 Mbps at $Q_T = 6$ dB and $Q_R = 3$ dB.

VII. CONCLUSION

In this paper, we characterize a two tier network, consisting of classical sub-6GHz macro cells, and Multi RAT small cells, able to operate in sub-6GHz and mm-wave bands. First, we propose a two-step tier and RAT selection strategy where the sub-6GHz band is used to speed-up the initial access procedure in the mm-wave RAT, and then we investigate the effect of tier and RAT offloading in terms of SINR, cell load, and throughput. Our study highlights the fundamental trade-offs between outage probability, user throughput, and overloading probability, and, thereby, underscores the necessity of the dual band small cells to maintain outage below a certain threshold, specially in sparse deployments. In our system model, we have proposed effective approaches to optimize the user association. However, obtaining closed form solutions for the optimal biases and the maximum traffic density that the network can handle are open challenges. Moreover, the dual band
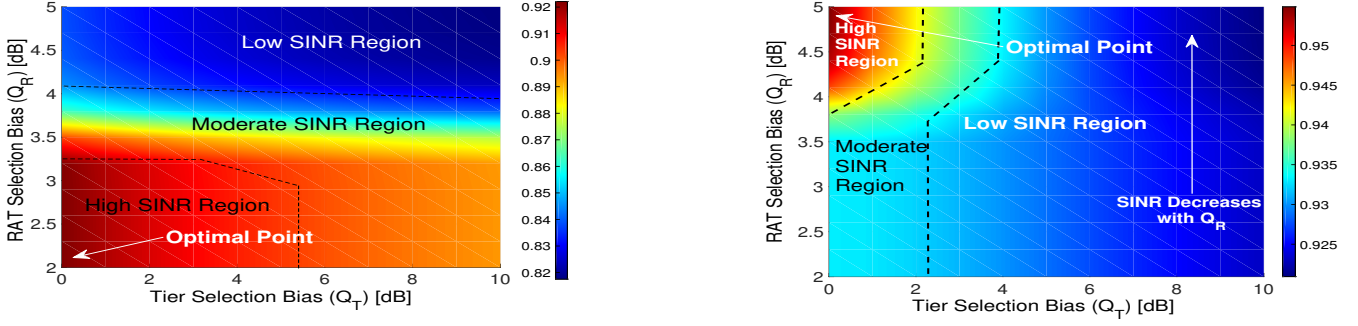
Figure 6: SINR coverage probability as a function of Q_T and Q_R at a threshold of $\gamma = -10$ dB for $d_M = 200$ m, $d_S = 20$ m for left) $\lambda_S/\lambda_M = 50$ right) $\lambda_S/\lambda_M = 200$.
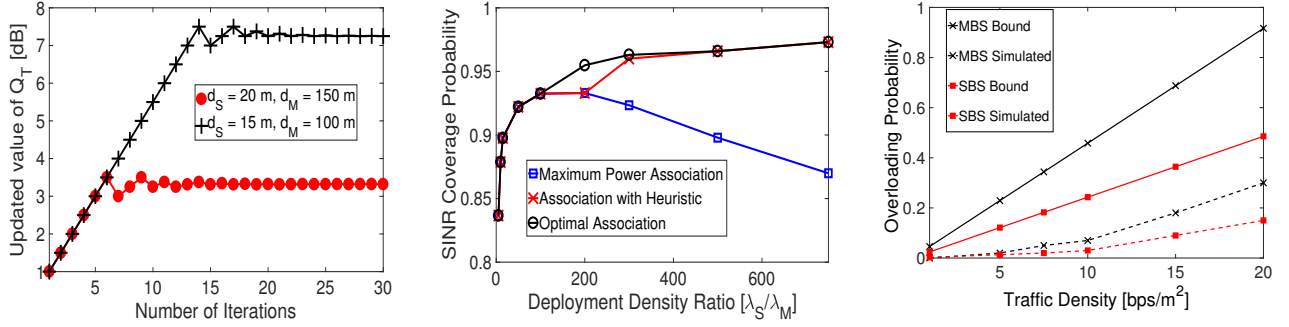

Figure 7: left) Convergence of gradient descent algorithm for $\lambda_S/\lambda_M = 100, d_S = 10$ m and $d_M = 100$ m; center) Comparison of RAT selection strategies; right) Tightness of the bound on probability of overloading.
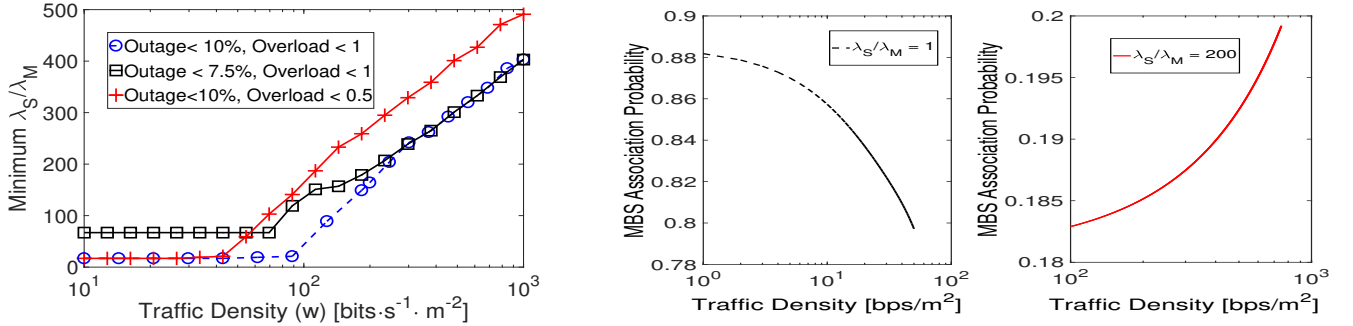

Figure 8: left) Minimum required deployment density for a given traffic density and right) Throughput optimal MBS association probabilities.
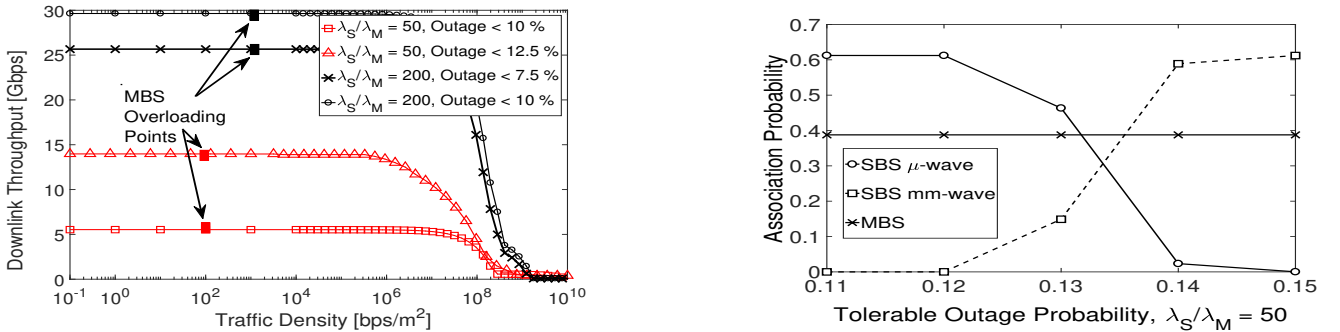

Figure 9: left) Optimal downlink user throughput and right) Optimal association probabilities for different outage probability constraints.
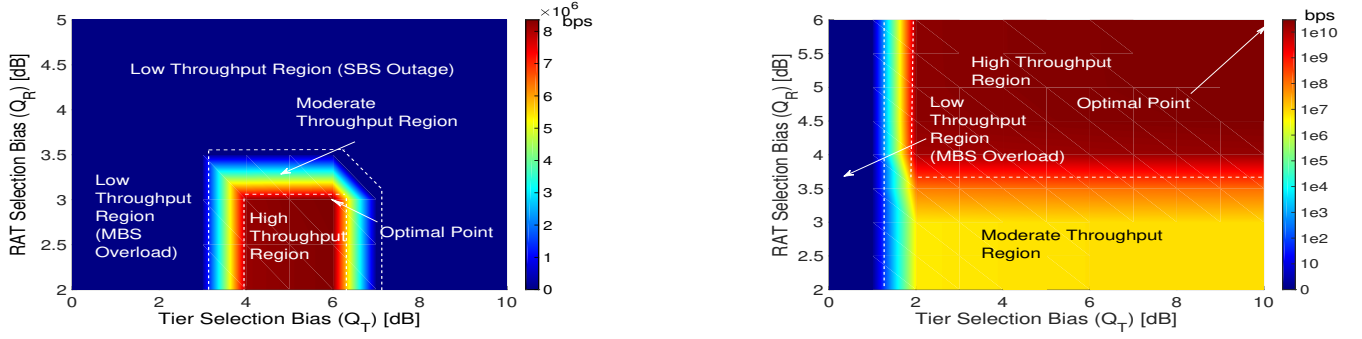
Figure 10: Effective user throughput vs Q_T and Q_R at a traffic density of 100 bits·s^{-1}m^{-2}, tolerable outage probability of 0.10, $d_M = 200$ m, $d_S = 20$ m for left) $\lambda_S/\lambda_M = 50$ right) $\lambda_S/\lambda_M = 200$.

nature of the base stations calls for advanced radio resource management, which is an interesting topic to be investigated.

APPENDIX A
TIER SELECTION PROBABILITY

The probabilities that at least one LOS MBS and LOS SBS exist are, respectively, $\mathbb{E}[\mathbb{1}(t_M L)] = 1 - \exp(-\pi\lambda_M d_M^2)$ and $\mathbb{E}[\mathbb{1}(t_S L)] = 1 - \exp(-\pi\lambda_S d_S^2)$. Then, the values of $\mathbb{P}(\tilde{Q}_T P_{tv\mu 1} > \tilde{Q}_T P_{t'v\mu 1})$ are derived as follows:

$$\mathbb{P}(P_{ML\mu 1} > Q_T \cdot P_{SL\mu 1})$$

$$= \int_0^\infty e^{-\Lambda'_{SL\mu}(0, Q_T r)} e^{-\Lambda'_{ML\mu}(0, r)} \lambda'_{ML\mu}(r) dr$$

$$= \int_0^{\frac{d_S^{\alpha_{SL\mu}}}{Q_T \cdot K_{SL\mu} P_S}} e^{-\Lambda'_{SL\mu}(0, Q_T r)} e^{-\Lambda'_{ML\mu}(0, r)} \lambda'_{ML\mu}(r) dr +$$

$$\int_{\frac{d_S^{\alpha_{SL\mu}}}{Q_T \cdot K_{ML\mu} P_S}}^{\frac{d_M^{\alpha_{ML\mu}}}{K_{SL\mu} P_M}} e^{-\Lambda'_{SL\mu}\left(0, \frac{d_S^{\alpha_{SL\mu}}}{K_{SL\mu} P_S}\right)} e^{-\Lambda'_{ML\mu}(0, r)} \lambda'_{ML\mu}(r) dr$$

$$= \frac{1}{1 + K_1}(1 - e^{-(K_1 + 1)t_1}) + e^{-\Lambda'_{SL\mu}\left(0, \frac{d_S^{\alpha_{SL\mu}}}{K_{SL\mu} P_S}\right)}.$$

$$\left[\exp\left(-\Lambda'_{ML\mu}\left(0, \frac{d_S^{\alpha_{SL\mu}}}{Q_T K_{SL\mu} P_S}\right)\right) - \exp\left(-\Lambda'_{ML\mu}\left(0, \frac{d_M^{\alpha_{ML\mu}}}{K_{ML\mu} P_M}\right)\right) \right],$$

where, $K_1 = \pi\lambda_S \left(\frac{K_{SL\mu} P_S Q_T}{P_M}\right)^{\frac{2}{\alpha_{SL\mu}}} (\pi\lambda_M)^{-\frac{\alpha_{ML\mu}}{\alpha_{SL\mu}}}$ and $t_1 = \pi\lambda_M (K_{ML\mu} P_M)^{\frac{2}{\alpha_{ML\mu}}} \left(\frac{d_S^{\alpha_{SL\mu}}}{Q_T K_{SL\mu} P_S}\right)^{\frac{2}{\alpha_{ML\mu}}}$. Similarly,

$$\mathbb{P}(P_{MN\mu 1} > Q_T \cdot P_{SN\mu 1})$$

$$= \exp\left(-\Lambda'_{SN\mu}\left(0, \frac{d_S^{\alpha_{SN\mu}}}{K_{SN\mu} P_S}\right)\right) \frac{e^{-(K_2 + 1)t_2}}{1 + K_2},$$

where $K_2 = \pi\lambda_S \left(\frac{K_{SN\mu} P_S Q_T}{K_{MN\mu} P_M}\right)^{\frac{2}{\alpha_{SN\mu}}} (\pi\lambda_M)^{-\frac{\alpha_{MN\mu}}{\alpha_{SN\mu}}}$ and $t_2 = \pi\lambda_M d_M^2 (K_{MN\mu} P_M)^{\frac{2}{\alpha_{MN\mu}} - 1}$. Finally,

$$\mathbb{P}(Q_T \cdot P_{SL\mu 1} > P_{ML\mu 1}) = 1 - \mathbb{P}(P_{ML\mu 1} > Q_T \cdot P_{SL\mu 1});$$
$$\mathbb{P}(Q_T \cdot P_{SN\mu 1} > P_{MN\mu 1}) = 1 - \mathbb{P}(P_{MN\mu 1} > Q_T \cdot P_{SN\mu 1}).$$

Using these expressions in Eq. (3) and Eq. (4) completes the proof.

APPENDIX B
RAT SELECTION PROBABILITY

The power received from strongest SBS of state v is $P_{Sv\mu 1} = (\xi_{Sv\mu 1})^{-1} = K_{Sv\mu} P_S ||x_{Sv1}||^{-\alpha_{Sv\mu}}$.

So, the estimate of the mm-wave power is: $P_{Svm1} = G_0 K_{SLm} P_S ||x_{Sv1}||^{-\alpha_{Svm}}$. Therefore the probability of sub-6GHz service, given that the user is associated with strongest SBS of visibility state v, is calculated as:

$$\mathbb{P}_{v\mu} = \mathbb{P}(P_{Sv\mu 1} > Q_R \times P_{Svm1})$$

$$= \mathbb{P}\left(||x_{Sv1}|| \geq \left(\frac{K_{Svm} G_0 Q_R}{K_{Sv\mu}}\right)^{\frac{1}{\alpha_{Svm} - \alpha_{Sv\mu}}}\right)$$

$$= \exp\left(-\pi\lambda_S \left(\frac{K_{Svm} G_0 Q_R}{K_{Sv\mu}}\right)^{\frac{2}{\alpha_{vm} - \alpha_{v\mu}}}\right) \quad (19)$$

The probability of mm-wave service is given by $\mathbb{P}_{Svm} = 1 - \mathbb{P}_{Sv\mu}$. This completes the proof.

APPENDIX C
PROOF OF EQ. (15)

We provide the derivation only for the LOS MBS association case. The other cases follow similarly. When the user is associated with the strongest LOS MBS, it experiences interference from the other LOS MBSs, the NLOS MBSs, and the SBSs. Thus, the instantaneous SINR is:

$$SINR_{ML\mu} = \frac{h_{\xi_{ML\mu 1}}(\xi_{ML\mu 1})^{-1}}{I_{ML\mu} + I_{MN\mu} + I_{SL\mu} + I_{SN\mu} + \sigma_N^2},$$

where $I_{\{.\}}$ denote the interference terms given as

$$I_{ML\mu} = \sum_{\xi_{ML\mu i} \in \phi'_{ML\mu} \setminus \{\xi_{ML\mu 1}\}} h_{\xi_{ML\mu i}}(\xi_{ML\mu i})^{-1};$$

$$I_{MN\mu} = \sum_{\xi_{MN\mu i} \in \phi'_{MN}} h_{\xi_{MN\mu i}}(\xi_{MN\mu i})^{-1};$$

$$I_{SL\mu} = \sum_{\xi_{SL\mu i} \in \phi'_{SL\mu}} h_{\xi_{SL\mu i}}(\xi_{SL\mu i})^{-1};$$

$$I_{SN\mu} = \sum_{\xi_{SN\mu i} \in \phi'_{SN\mu}} h_{\xi_{SN\mu i}}(\xi_{SN\mu i})^{-1}.$$

Now,

$$
\begin{aligned}
\mathbb{P}_{CML\mu} &= \mathbb{P}(SINR_{ML\mu} > \gamma) \\
&= \mathbb{P}\left(\frac{h_{\xi_{ML\mu 1}}(\xi_{ML\mu 1})^{-1}}{I_{ML\mu} + I_{MN\mu} + I_{SL\mu} + I_{SN\mu} + \sigma_N^2} > \gamma\right) \\
&= \mathbb{P}\left(h_{\xi_{ML\mu 1}} > \frac{\gamma(I_{ML\mu} + I_{MN\mu} + I_{SL\mu} + I_{SN\mu} + \sigma_N^2)}{(\xi_{ML\mu 1})^{-1}}\right) \\
&\overset{(a)}{=} \mathbb{E}_{\xi_{ML\mu 1}}\left\{\mathbb{E}_{\phi'_{ML\mu}}\left[\exp\left(-\frac{\gamma \cdot I_{ML\mu}}{(\xi_{ML\mu 1})^{-1}}\right)\right].\right.
\end{aligned}
$$

$$
\mathbb{E}_{\phi'_{MN\mu}}\left[\exp\left(-\frac{\gamma \cdot I_{MN\mu}}{(\xi_{ML\mu 1})^{-1}}\right)\right].
$$

$$
\mathbb{E}_{\phi'_{SL\mu}}\left[\exp\left(-\frac{\gamma \cdot I_{SL\mu}}{(\xi_{ML\mu 1})^{-1}}\right)\right].
$$

$$
\left.\mathbb{E}_{\phi'_{SN\mu}}\left[\exp\left(-\frac{\gamma \cdot I_{SN\mu}}{(\xi_{ML\mu 1})^{-1}}\right)\right]\left(\exp\left(-\frac{\gamma \cdot \sigma_N^2}{(\xi_{ML\mu 1})^{-1}}\right)\right)\right\},
$$

$$\tag{20}$$

where (a) comes from the pdf of $h_{\xi_{ML\mu 1}}$. Now,

$$
\begin{aligned}
&\mathbb{E}_{\phi'_{ML\mu}}\left[\exp\left(-\frac{\gamma \cdot I_{ML\mu}}{(\xi_{ML\mu 1})^{-1}}\right)\right] = \\
&\mathbb{E}\left[\exp\left(-\frac{\gamma \cdot \sum_{\phi'_{ML\mu}\backslash\{\xi_{ML\mu 1}\}} h_y y^{-1}}{(\xi_{ML\mu i})^{-1}}\right)\right] \\
&= \mathbb{E}\left[\prod_{\phi'_{ML\mu}\backslash\{\xi_{ML\mu 1}\}} \mathbb{E}_{h_y}\left[\exp\left(-\frac{\gamma \cdot h_y(y)^{-1}}{(\xi_{ML\mu 1})^{-1}}\right)\right]\right] \\
&= \exp\left(-\int_{\xi_{ML\mu 1}}^{\infty}\left(1 - \mathbb{E}_{h_y}\left[\exp\left(-\frac{\gamma \cdot h_y y^{-1}}{(\xi_{ML\mu 1})^{-1}}\right)\right]\right)\right. \cdot \\
&\qquad\qquad \left.\Lambda'_{ML\mu}(dy)\right) \\
&= \exp\left(-\int_{\xi_{ML\mu 1}}^{\infty}\left(\frac{\gamma\xi_{ML\mu 1}}{y + \gamma\xi_{ML\mu 1}}\Lambda'_{ML\mu}(dy)\right)\right).
\end{aligned}
$$

Similarly,

$$
\begin{aligned}
&\mathbb{E}_{\phi'_{tv\mu}}\left[\exp\left(-\frac{\gamma \cdot I_{tv\mu}}{(\xi_{ML\mu 1})^{-1}}\right)\right] = \\
&\qquad \exp\left(-\int_{l_{tv}}^{\infty}\left(1 - \frac{y}{y + \gamma\xi_{ML\mu 1}}\Lambda'_{tv\mu}(dy)\right)\right),
\end{aligned}
$$

for $tv = MN, SL$ and SN, respectively, where the lower indexes are: $l_{SL} = l_{SN} = Q_T \cdot \xi_{ML\mu 1}$ and $l_{MN} = \xi_{ML\mu 1}$. Substituting the above results in Eq. (20), and taking the expectation with respect to $\xi_{ML\mu 1}$, completes the proof.

APPENDIX D
PROOF OF PROPOSITION 1

Consider two LOS SBS S_1 and S_2[5]. Let the power received by the typical user from the SBS S_1 in mm-wave and sub-

---

[5]The analysis where there are NLOS SBS can be performed with similar reasoning.

6Ghz band be P_{S1m} and $P_{S1\mu}$, respectively. Let the corresponding values for S_2 be P_{S2m} and $P_{S2\mu}$, respectively. Now

$$
\begin{aligned}
P_{S1\mu} \geq P_{S2\mu} &\iff K_\mu P_S d_1^{\alpha_{Sv\mu}} \geq K_\mu P_S d_2^{\alpha_{Sv\mu}} \\
&\iff K_m P_S d_1^{\alpha_{Svm}} \geq K_m P_S d_2^{\alpha_{Svm}} \\
&\iff P_{S1m} \geq P_{S2m} \\
&\iff Q_R P_{S1m} \geq Q_R P_{S2m} \tag{21}
\end{aligned}
$$

APPENDIX E
PROBABILITY OF SUB-OPTIMAL ASSOCIATION

Recall that E_1 and E_2 denote the events the biased received power from the strongest SBS (denoted S_1) in sub-6GHz band is less than that received from the strongest MBS (denoted by M_1) and the biased received power from S_1 in mm-wave is higher than the received power from M_1, respectively. We have:

$$
\mathbb{P}\left[E_2 \mid E_1\right] = \frac{\mathbb{P}\left[E_2 \cap E_1\right]}{\mathbb{P}\left[E_1\right]} =
$$

$$
\frac{1}{\mathbb{P}\left[P_M d_{M1}^{-\alpha_{Mv'\mu}} \geq Q_T P_S d_{S1}^{-\alpha_{Sv\mu}}\right]} \cdot
$$

$$
\left(\mathbb{P}\left[K_m P_S Q_R Q_T G_0 d_{S1}^{-\alpha_{Svm}} \geq K_\mu P_M d_{M1}^{-\alpha_{Mv'\mu}} \cap\right.\right.
$$

$$
\left.\left. P_M d_{M1}^{-\alpha_{Mv'\mu}} \geq Q_T P_S d_{S1}^{-\alpha_{Sv\mu}}\right]\right)
$$

$$
= \frac{1}{\mathbb{P}\left[d_{S1} \geq \left(\frac{P_S Q_T}{P_M} d_{M1}^{\alpha_{Mv'\mu}}\right)^{\frac{1}{\alpha_{Sv\mu}}}\right]} \cdot
$$

$$
\mathbb{P}\left[d_{S1} < \left(\frac{K_m P_S Q_R Q_T G_0}{K_\mu P_M} d_{M1}^{\alpha_{Mv'\mu}}\right)^{\frac{1}{\alpha_{Svm}}} \cap\right.
$$

$$
\left. d_{S1} \geq \left(\frac{P_S Q_T}{P_M} d_{M1}^{\alpha_{Mv'\mu}}\right)^{\frac{1}{\alpha_{Sv\mu}}}\right]
$$

$$
= \mathbb{E}_{d_{M1}}\left[\frac{1}{\exp\left(-\pi\lambda_S\left(\zeta_1 x^{\alpha_{Mv'\mu}}\right)^{\frac{2}{\alpha_{Sv\mu}}}\right)} \cdot \right.
$$

$$
\left.\left(\exp\left(-\pi\lambda_S\left(\left(\zeta_2 x^{\alpha_{Mv'\mu}}\right)^{\frac{2}{\alpha_{Svm}}} - \left(\zeta_1 x^{\alpha_{Mv'\mu}}\right)^{\frac{2}{\alpha_{Sv\mu}}}\right)\right)\right)\right]
$$

$$
= 2\pi\lambda_M \cdot
$$

$$
\int_0^{d_M} \frac{\exp\left(-\pi\lambda_S\left(\left(\zeta_2 x^{\alpha_{Mv'\mu}}\right)^{\frac{2}{\alpha_{Svm}}} - \left(\zeta_1 x^{\alpha_{Mv'\mu}}\right)^{\frac{2}{\alpha_{Sv\mu}}}\right)\right)}{\exp\left(-\pi\lambda_S\left(\zeta_1 x^{\alpha_{Mv'\mu}}\right)^{\frac{2}{\alpha_{Sv\mu}}}\right)} \cdot
$$

$$
x\exp(-\pi\lambda_M x^2)dx
$$

Solving this integral with the approximated values of the path-loss exponents completes the proof.

REFERENCES

[1] J. G. Andrews, *et al.*, "What Will 5G Be?" *IEEE J. Sel. Areas Commun.*, vol. 32, no. 6, pp. 1065–1082, 2014.
[2] D. López-Pérez, *et al.*, "Towards 1 Gbps/UE in Cellular Systems: Understanding Ultra-Dense Small Cell Deployments," *IEEE Commun. Surveys Tuts.*, vol. 17, no. 4, pp. 2078–2101, 2015.
[3] T. S. Rappaport, *et al.*, "Millimeter Wave Mobile Communications for 5G Cellular: It Will Work!" *IEEE Access*, vol. 1, pp. 335–349, 2013.

[4] K. Okino, *et al.*, "Pico Cell Range Expansion with Interference Mitigation toward LTE-Advanced Heterogeneous Networks," in *IEEE ICC Workshops*, 2011, pp. 1–5.

[5] M. Eguizabal and A. Hernandez, "Interference management and cell range expansion analysis for LTE picocell deployments," in *IEEE PIMRC*, 2013, pp. 1592–1597.

[6] M. S. Ali, P. Coucheney, and M. Coupechoux, "Load balancing in heterogeneous networks based on distributed learning in potential games," in *IEEE WiOpt*, 2015, pp. 371–378.

[7] A. Ghosh, *et al.*, "Millimeter-Wave Enhanced Local Area Systems: A High-Data-Rate Approach for Future Wireless Networks," *IEEE J. Sel. Areas Commun.*, vol. 32, no. 6, pp. 1152–1163, 2014.

[8] 3GPP TSG RAN, "TR 38.900, Study on channel model for frequency spectrum above 6 GHz," *v14.1.0*, September 2016.

[9] White Paper, "5G Channel Model for bands up to 100 GHz," *http://www.5gworkshops.com/5gcm.html*.

[10] Y. Li, *et al.*, "On the initial access design in millimeter wave cellular networks," in *IEEE GLOBECOM Wkshps.*, 2016, pp. 1–6.

[11] H2020-ICT-671650 mmMAGIC, "D3.1: Initial concepts on 5G architecture and integration," *Available Online at https://5g-mmmagic.eu/*, Mar. 2016.

[12] A. Kangas and T. Wigren, "Angle of arrival localization in LTE using MIMO pre-coder index feedback," *IEEE Commun. Lett.*, vol. 17, no. 8, pp. 1584–1587, 2013.

[13] S. Onoe, "Evolution of 5G mobile technology toward 2020 and beyond," in *IEEE ISSCC*, 2016, pp. 23–28.

[14] Z. Pi and F. Khan, "An introduction to millimeter-wave mobile broadband systems," *IEEE Commun. Mag.*, vol. 49, no. 6, pp. 101–107, June 2011.

[15] H. ElSawy, E. Hossain, and M. Haenggi, "Stochastic Geometry for Modeling, Analysis, and Design of Multi-Tier and Cognitive Cellular Wireless Networks: A Survey," *IEEE Commun. Surveys Tuts.*, vol. 15, no. 3, pp. 996–1019, 2013.

[16] T. Bai and R. W. Heath, "Coverage and Rate Analysis for Millimeter-Wave Cellular Networks," *IEEE Trans. Wireless Commun.*, vol. 14, no. 2, pp. 1100–1114, 2015.

[17] S. Singh and J. G. Andrews, "Joint Resource Partitioning and Offloading in Heterogeneous Cellular Networks," *IEEE Trans. Wireless Commun.*, vol. 13, no. 2, pp. 888–901, 2014.

[18] M. Di Renzo, "Stochastic Geometry Modeling and Analysis of Multi-Tier Millimeter Wave Cellular Networks," *IEEE Trans. Wireless Commun.*, vol. 14, no. 9, pp. 5038–5057, 2015.

[19] M. S. Omar, *et al.*, "Performance analysis of hybrid 5g cellular networks exploiting mmwave capabilities in suburban areas," in *IEEE ICC*, 2016, pp. 1–6.

[20] G. Yao, *et al.*, "Coverage and rate analysis for non-uniform millimeter-wave heterogeneous cellular network," in *8th IEEE WCSP, 2016*, 2016, pp. 1–6.

[21] H. Elshaer, *et al.*, "Downlink and Uplink Cell Association With Traditional Macrocells and Millimeter Wave Small Cells," *IEEE Trans. Wireless Commun.*, vol. 15, no. 9, pp. 6244–6258, Sept. 2016.

[22] T. Bonald and A. Proutière, "Wireless Downlink Data Channels: User Performance and Cell Dimensioning," in *ACM MobiCom*, 2003, pp. 339–352.

[23] B. Błaszczyszyn, M. Jovanovicy, and M. K. Karray, "How user throughput depends on the traffic demand in large cellular networks," in *IEEE WiOpt*, 2014, pp. 611–619.

[24] S. Singh, H. S. Dhillon, and J. G. Andrews, "Offloading in heterogeneous networks: Modeling, analysis, and design insights," *IEEE Trans. Wireless Commun.*, vol. 12, no. 5, pp. 2484–2497, 2013.

[25] T. Bai, R. Vaze, and R. W. Heath, "Analysis of Blockage Effects on Urban Cellular Networks," *IEEE Trans. Wireless Commun.*, vol. 13, no. 9, pp. 5070–5083, 2014.

[26] 3GPP, "TR 36.873, Study on 3D channel model for LTE," *Release 12*, March 2010.

[27] 3GPP TSG RAN, "TR 36.814, E-UTRA; Further advancements for E-UTRA physical layer aspects," *v9.0.0*, March 2010.

[28] X. Zhang and M. Haenggi, "A Stochastic Geometry Analysis of Inter-Cell Interference Coordination and Intra-Cell Diversity," *IEEE Trans. Wireless Commun.*, vol. 13, no. 12, pp. 6655–6669, 2014.

[29] H. Shokri-Ghadikolaei, *et al.*, "Millimeter Wave Cellular Networks: A MAC Layer Perspective," *IEEE Trans. Commun.*, vol. 63, no. 10, pp. 3437–3458, 2015.

[30] G. Ghatak, A. De Domenico, and M. Coupechoux, "Performance Analysis of Two-tier Networks with Closed Access Small-cells," in *IEEE WiOpt*, 2016, pp. 1–8.

[31] A. Leon-Garcia, *Probability, statistics, and random processes for electrical engineering*. Pearson/Prentice Hall, 3rd ed., 2008.

[32] S. M. Hasan, M. A. Hayat, and M. F. Hossain, "On the downlink SINR and outage probability of stochastic geometry based LTE cellular networks with multi-class services," in *18th ICCIT*, Dec 2015, pp. 65–69.

Gourab Ghatak received his BTech degree (2013) from National Institute of Technology (NIT) Durgapur, India, and MTech degree (2015) from Indian Institute of Technology (IIT) Kanpur, India, respectively. He completed his MTech thesis as a DAAD research scholar (2014-2015) at the Vodafone Chair Mobile Communications Systems, Technische Universität (TU) Dresden, Germany, where he worked on channel estimation schemes for GFDM. He is currently working towards his PhD degree in CEA, Leti, France and in Université Paris Saclay, France. His research interests include stochastic geometry, millimeter-wave communications, 5G network planning, and signal processing for 5G waveforms.

Dr. Antonio De Domenico received his M.Sc. and Ph.D. degrees in telecommunication engineering in 2008 and 2012 from the University of Rome "La Sapienza" and the University of Grenoble, respectively. Since 2009, he has worked with the CEA-LETI – MINATEC, Grenoble, France, as a research engineer. His research topics are cloud-enabled heterogeneous wireless networks, millimeter-wave-based communications, machine learning, and green communications. He is the main inventor or co-inventor of nine patents. In 2017, Antonio has been awarded by the CEA Enhanced Eurotalents Programme, and he is currently a visiting researcher in the Communications Group of the Department of Electrical and Computer Engineering at the University of Toronto.

Marceau Coupechoux is Professor at Telecom ParisTech and Professeur Chargé de Cours at Ecole Polytechnique. He obtained his Master from Telecom ParisTech (1999) and from University of Stuttgart (2000), his Ph.D. from Institut Eurecom (2004), his Habilitation from University Pierre et Marie Curie (2015). From 2000 to 2005, he was with Alcatel-Lucent (in Bell Labs former Research & Innovation and then in the Network Design department). He was Visiting Scientist at the Indian Institute of Science, Bangalore, India, in 2011-2012. He has been General Co-Chair of WiOpt 2017. In the Computer and Network Science department of Telecom ParisTech, he is working on cellular networks, wireless networks, ad hoc networks, cognitive networks, internet of things, focusing mainly on performance evaluation, optimization and resource management.